The Astronomical Journal, 159:59 (12pp), 2020 February https://doi.org/10.3847/1538-3881/ab5f0b
© 2020. The American Astronomical Society. All rights reserved.

A Study of the Blue Straggler Population of the Old Open Cluster Collinder 261

M. J. Rain[1], G. Carraro[1], J. A. Ahumada[2], S. Villanova[3], H. Boffin[4,5], L. Monaco[6], and G. Beccari[5]
[1] Dipartimento di Fisica e Astronomia, Universita di Padova, Vicolo Osservatorio 3, I-35122, Padova, Italy
[2] Observatorio Astronómico, Universidad Nacional de Córdoba, Laprida 854, 5000 Córdoba, Argentina
[3] Departamento de Astronomía, Universidad de Concepción, 169 Casilla, Concepción, Chile
[4] ESO, Alonso de Cordova 3107, Santiago de Chile, Chile
[5] ESO, Karl-Schwarzschild Strasse 2, D-85748 Garching, Germany
[6] Departamento de Ciencias Físicas, Universidad Andrés Bello, República 220, 837-0134 Santiago, Chile
Received 2019 September 20; revised 2019 November 25; accepted 2019 December 3; published 2020 January 20

Abstract

Blue stragglers (BSs) are stars located in an unexpected region of the color–magnitude diagram (CMD) of a stellar population, as they appear bluer and more luminous than the stars in the turn-off region. They are ubiquitous, since they have been found among Milky Way field stars, in open and globular clusters, and also in other galaxies of the Local Group. Here we present a study on the BS population of the old and metal-rich open cluster Collinder 261, based on *Gaia* DR2 data and on a multi-epoch radial velocity survey conducted with Fibre Large Array Multi Element Spectrograph (FLAMES) at the Very Large Telescope (VLT). We also analyze the radial distribution of the BS population to probe the dynamical status of the cluster. BS candidates were identified first with *Gaia* DR2, according to their position on the CMD, proper motions, and parallaxes. Their radial distribution was compared with those of main sequence, red giant, and red clump stars, to evaluate mass segregation. Additionally, their radial velocities (and the associated uncertainties) were compared with the mean radial velocity and velocity dispersion of the cluster. When possible, close binaries and long-period binaries were also identified, based on the radial velocity variations for the different epochs. We also looked for yellow stragglers, i.e., possible evolved BSs. We found 53 BS members of Collinder 261, six of them were already identified in previous catalogs. Among the BS candidates with radial velocity measurements, we found one long-period binary, five close-binary systems, three nonvariable stars; we also identified one yellow straggler.

Unified Astronomy Thesaurus concepts: Open star clusters (1160)

1. Introduction

Blue stragglers (BSs) are stars located in an unexpected region of the color–magnitude diagram (CMD) of a relatively old stellar population, since they appear bluer and more luminous than stars in the turn-off (TO) region. Their existence is incompatible with the standard stellar evolution theory, which predicts that stars in this region of the CMD should have already left the main sequence (MS) because of their mass. Thus, these stars somehow managed to gain mass and become a "rejuvenated" object. The formation mechanisms for the BSs are not yet fully understood; however, at present, there are two main leading scenarios: BSs could be the products of either direct stellar collisions (Hills & Day 1976), or mass-transfer activity in close-binary systems (McCrea 1964). Therefore, BSs can give information about the dynamical history of the cluster, the role of the dynamics on stellar evolution, the frequency of binary systems, and the contribution of binaries to cluster evolution. Hence, BSs certainly represent the link between standard stellar evolution and cluster dynamics. Additionally, they are rather ubiquitous as they have been found in all kinds of stellar environments: in the field, in open and globular clusters (GSs), and in galaxies of the Local Group. An extensive review of their properties has been presented by Boffin et al. (2014).

Open clusters seem to be stellar systems where BSs find themselves particularly comfortable. The reason for this is not yet clear and deserves more attention. The study of BS stars in open clusters is still limited to just a few cases, preventing their use as potential dynamical clocks, as it has been done in GC environments (Dalessandro 2014). Ferraro et al. (2012, hereafter, F12) showed that GCs can be grouped into three different families based on the radial profile of their BS distributions. Clusters of Family I, or dynamically young GCs, show a flat distribution; in these systems the dynamical friction has not yet caused visible effects, even in the innermost regions. In Family II GCs, the dynamical friction has become more efficient and the mass segregation has started, which has led to the presence of a peak at the center, and a minimum at small radii of the BS distribution. The outskirts of Family II clusters have still not been affected by the dynamical friction, i.e., it has not reached the most remote BSs, and therefore there is a rise of the BS density in these outer regions. Bhattacharya et al. (2019) recently studied the radial distribution of the very old open cluster Berkeley 17 (∼10 Gyr; Kaluzny 1994), and placed it in the Family II class of GCs. Finally, when the system is highly evolved, the external maximum disappears, and the only noticeable peak in the distribution is the central one; GCs showing this profile are grouped in the Family III.

A few catalogs of BS stars in open clusters are available, but they are based on a purely photometric selection (de Marchi et al. 2006; Ahumada & Lapasset 2007, hereafter d06 and AL07). While useful, the photometric selection is not reliable enough to allow the derivation of statistical properties of BS stars, since their membership is uncertain and field stars tend to occupy the very same region of BS stars in the CMD (Carraro et al. 2008). Only an accurate membership assessment may let us know the real number of BS stars in a given cluster, and the evolutionary status of each of them. So far, this has been done only for a handful of clusters. A very well studied cluster is M67, which harbors 24 BS stars (Leonard 1996 and references therein). In this respect, however, perhaps the

Table 1
Main Parameters of Collinder 261

l^a (deg)	b^a (deg)	Distance[b] (kpc)	$E(B-V)^a$ (mag)	$R_c^{1,c}$ (arcmin)	$R_h^{2,c}$ (arcmin)	$R_a^{1,a}$ (arcmin)	log(age)[a] (yr)	[Fe/H] (dex)	RV[d] (km s^{-1})
301.68	−0.53	2.9	0.27	2.6	6.4	9.0	9.95	-0.01 ± 0.11	-25.44 ± 0.93

Note. [1]Core radius. [2]Half-mass–radius. [3]Apparent radius.
References. [a] Dias et al. (2002), [b] Cantat-Gaudin et al. (2018), [c] Vats & van den Berg (2017), and [d] Mishenina et al. (2015).

best-studied case is NGC 188 (Geller et al. 2010; Geller & Mathieu 2011; Geller et al. 2013). These authors have found 21 bona fide BS stars, with a binary fraction of 76% ± 19%. Among the 21 BSs, only four do not show velocity variations, although it cannot be discarded that they might be long-period variables ($P > 3000$ days), or that they are being seen pole-on. Some binary BSs in open clusters belong to very long-period systems, and hence are difficult to detect spectroscopically and almost impossible to detect photometrically. The percentage of binaries among BS stars is significantly larger than in the cluster MS, where it is of about 20% (Mathieu & Geller 2009; Geller & Mathieu 2012). For all the BS binaries, the cited works derive period solutions. They find that the orbital period distribution of BS stars is quite different from that of MS binaries, with the majority of BS having orbital periods close to 1000 days, with most of them likely having a white dwarf companion. Recently, white dwarf companions have been detected for seven BSs in NGC 188 using far-ultraviolet *Hubble Space Telescope* (*HST*) observations (Gosnell et al. 2015). Similarly, five of the six binary BSs of M67 have periods from 800 to 5000 days (Latham & Milone 1996; Pribulla et al. 2008). Besides these two clusters, spectroscopic studies of BSs in open clusters are available only for individual stars, for example: NGC 6791 (Brogaard et al. 2018); NGC 6087, NGC 6087, NGC 6530, and Collinder 223 (Aidelman et al. 2018); and NGC 2141 (Luo 2015).

Collinder 261, or Harvard 6 (C1234−682, $\alpha = 12^h37^m57^s$, $\delta = -68°22'00''$, J2000.0), is one of the oldest open clusters of the Milky Way, having an age from 7 to 9.3 Gyr (Bragaglia & Tosi 2006; Dias et al. 2002). The cluster metallicity is close to solar, and reported values for the distance lie between 2.2 and 2.9 kpc, while its reddening $E(B-V)$ has been estimated between 0.25 and 0.34 mag (Mazur et al. 1995; Gozzoli et al. 1996; Bragaglia & Tosi 2006; Dias et al. 2002; Cantat-Gaudin et al. 2018). The cluster parameters are summarized in Table 1. Due to the cluster location toward the galactic center, its CMD is heavily contaminated by field stars. In this sense, the second and latest data release of *Gaia* (DR2), which provides precise five-parameter astrometry (positions, parallaxes, and proper motions), as well as three-band photometry (G, G_{BP}, and G_{RP} magnitudes) for more than one billion stars (Lindegren et al. 2018), allows a proper study of Collinder 261 members and the BS population with great confidence. Gao (2018) and Cantat-Gaudin et al. (2018, hereafter CG18) estimate ∼2000 members on the Collinder 261 area by applying the unsupervised clustering technique on the *Gaia* data.

The layout of the paper is as follows. In Section 2 we present the data sets used in this work. In Section 3 we describe the photometric analysis and the selection criteria of BS stars in open clusters and the results of such selection for Collinder 261. Section 4 explains how the spectra were reduced and the radial velocities extracted; in this section we also define the criteria to establish membership and binary status of our targets. In Section 5 we discuss the results of the photometric and spectroscopic detection. Finally, in Section 6, after a brief summary we give the conclusions of this study.

2. Data Sets

2.1. Photometric Data

We used the Data Release 2 Archive[7] of the European Space Agency mission *Gaia* (Gaia Collaboration et al. 2016, 2018). For more than a billion stars, this survey provides a five-parameter astrometric solution: position, trigonometric parallax, and proper motion, as well as photometry in three broadband filters (G, G_{BP}, and G_{RP}). The *Gaia* catalog also gives radial velocities for about 7 million stars, mostly brighter than $G \sim 13$. The astrometric solution, the photometric contents and validation, and the properties and validation of radial velocities are described in Lindegren et al. (2018), Evans et al. (2018), and Katz et al. (2019), respectively.

2.2. Spectroscopic Data

Collinder 261 was observed with the Fibre Large Array Multi Element Spectrograph (FLAMES)[8] at the Very Large Telescope (VLT) of the European Southern Observatory (ESO; Paranal Observatory, Chile), using the combination of the mid-resolution spectrograph GIRAFFE and the fiber link UVES. The data were collected in two periods: 2011 October to 2012 March, and 2017 October to 2018 April, under ESO programs 088.D-0045(A) and 0100.D-0052(A).

The UVES fibers were allocated to the cluster's clump stars, whose membership is very solid, to set the zero-point of the radial velocity. The reduction and analysis of the UVES data are described by Mishenina et al. (2015). GIRAFFE was used with the setup HR8, which covers the wavelength range of 491.7–516.3 nm, with a spectral resolution of $R \equiv \lambda/\Delta\lambda \equiv 20,000$. The integration time was ∼2400 s for all spectra. In total, Collinder 261 was observed in four epochs; some details of the observations are given in Table 2. For the GIRAFFE data we just performed the sky-subtraction and normalization using the IRAF[9] packages `sarith` and `continuum`, since the data were already reduced in Phase 3.

3. Photometric Analysis

For our photometry-based analysis, we took advantage of the selection of cluster members already performed by CG18, who used the membership assignment code UPMASK[10] (Unsupervised Photometric Membership Assignment in Stellar Clusters;

[7] https://gea.esac.esa.int/archive/
[8] http://www.eso.org/sci/facilities/paranal/instruments/flames.html
[9] IRAF is distributed by the National Optical Astronomy Observatory, which is operated by the Association of Universities for Research in Astronomy, Inc.., under cooperative agreement with the National Science Foundation.
[10] https://cran.r-project.org/web/packages/UPMASK/index.html

Table 2
Details of the Spectroscopic Observations Carried out on 2012 February 24 and March 1–6, and 2018 February 3–4, with a Signal-to-noise Ratio between 15 and 120

Epoch	MJD_{start}[a] (days)	MJD_{end}[a] (days)	Exposure (s)
1	55982.277794959	55982.3055727877	2400.0044
2	55988.222295996	55988.2500738154	2400.0036
3	55993.234082174	55993.2618600004	2400.0042
4	58153.314142684	58153.3419204942	2400.0028

Note.
[a] Modified Julian date JD−24,00000.5.

Krone-Martins & Moitinho 2014). This procedure is based on proper motions and parallax selection criteria. They considered as cluster members those stars located over a radius twice as large as the value of $r_{DAML} = 9'$ reported by Dias et al. (2002, hereafter DAML02), with proper motions within 2 mas yr^{-1} and with parallaxes within 0.5 mas from the cluster centroid. In this way, they selected about 2000 members of Collinder 261. For every star they estimated a membership probability from 0 to 100%. To calculate the cluster mean proper motion and parallax, they used only stars with probabilities above 50%.

Cantat-Gaudin et al. (2018) report the mean values $\mu_\alpha \cos\delta = -6.35 \pm 0.16$ (0.004) mas yr^{-1}, $\mu_\alpha = -2.70 \pm 0.16$ (0.004) mas yr^{-1}, and $\varpi = 0.315 \pm 0.082$ (0.002) mas. Just to be cautious, we calculated our own proper motions values following a similar procedure as that of Bhattacharya et al. (2019). We employed the table access protocol and the astronomical data query language, together with the Tool for OPerations on Catalogs And Table (TOPCAT),[11] to access the *Gaia* data; for this, we identified the *Gaia* DR2 counterparts of confirmed Collinder 261 members, as follows. De Silva et al. (2007) measured radial velocities, metallicities, and chemical abundances (Mg, Si, Ca, Mn, Fe, Ni, Zr, and Ba) of 12 giant stars, and confirmed their membership; we cross-correlated the position on the sky of these stars and the *Gaia* DR2 catalog, looking for the nearest neighbors within 1″. Our mean proper motions and parallax values are: $\mu_\alpha \cos\delta = -6.35 \pm 0.13$ mas yr^{-1}, $\mu_\alpha = -2.73 \pm 0.14$ mas yr^{-1}, and $\varpi = 0.321 \pm 0.019$ mas, which are in complete agreement with those of CG18 and Gao (2018; $\mu_\alpha \cos\delta = -6.340 \pm 0.006$ mas yr^{-1}, $\mu_\alpha = -2.710 \pm 0.004$ mas yr^{-1}, and $\varpi = 0.3569 \pm 0.0027$ mas). On the other hand, even considering the errors, our results are far from the values given by DAML02, namely, $\mu_\alpha \cos\delta = -0.65 \pm 4.94$ mas yr^{-1} and $\mu_\alpha = -0.51 \pm 3.76$ mas yr^{-1}.

Arenou et al. (2018) report the differences between the average zero-points of proper motions and parallaxes from DAML02 and *Gaia* catalogs. They found $\mu_{Gaia} - \mu_{DAML02} = 0.0 \pm 0.19$ mas yr^{-1} and 0.41 ± 0.18 mas yr^{-1} for μ_α and $\mu_\alpha \cos\delta$ respectively, and $\varpi_{Gaia} - \varpi_{DAML02} = -0.064 \pm 0.17$ mas for the parallaxes. Arenou et al. (2018) do not find evidence for the presence of significant systematic errors in the *Gaia* DR2 proper motions. Therefore, the differences between our results and the published values of DAML02 seem unlikely to be caused by systematic errors in the *Gaia* data. Since our values were calculated using giant stars of confirmed membership, we suggest that the DAML02 proper motions might suffer from the lack of reliable cluster membership, as well as from significant contamination by field stars; these may be the main reasons of the discrepancies noted above.

[11] http://www.starlink.ac.uk/topcat/

3.1. Identification of the Stragglers

The region populated by the BSs in a CMD is well known today. According to Ahumada & Lapasset (1995, 2007) this area is delimited, to the left, by the zero-age main sequence (ZAMS); to the right, by the TO color; and down, by the magnitude at which the observed sequence of the cluster separates from the ZAMS. After applying a membership selection criterion, all stars falling in this region can be considered as genuine BSs with good certainty. Following AL07, we superimposed an 8.7 Gyr isochrone and a ZAMS of solar metallicity from Bressan et al. (2012), using $(m-M)_0 = 11.86$ and $E(B-V) = 0.27$, to the observed CMD (Figure 1). To not include spurious stars, we further constrained this region by plotting the equal-mass binary locus (dashed line) obtained by shifting the isochrone by 0.753 in G toward brighter magnitudes; in this way, we expect that binaries containing normal MS TO stars are excluded. These stars may appear as stragglers, but their components may not be such —see, e.g., Hurley & Tout (1998) for a discussion of this sequence.

Ahumada & Lapasset (2007) estimated a red limit of $(B-V) \simeq 0.86$ for the BS area of Collinder 261. To impose the same limit in the *Gaia* system, we used the relation of Jordi et al. (2010),

$$C_1 = 0.0187 + 1.6814\,C_2 - 0.3357\,C_2^2 + 0.117\,C_2^3. \quad (1)$$

With $C_2 = 0.86$, it result ass $C_1 = (G_{BP} - G_{RP}) = 1.20$. Stars redder than this limit can be considered as possible yellow stragglers.

Finally, we adopted an upper limit of 2.5 magnitudes above the TO for massive BSs.

In the top panel of Figure 1 we plotted the distribution of proper motions for stars in the Collinder 261 area. Gray dots represent *Gaia* DR2 stars within 15′ of the cluster center. Black filled circles are the cluster members of CG18. Light blue filled circles are the BS candidates, and orange filled circles are the yellow straggler candidates. In the bottom panel of Figure 1 we plotted the CMD of Collinder 261. The symbols are the same as the top panel. Open black circles are the BS candidates identified by AL07. Only 6 of 54 are classified as members according to *Gaia* data. The BS sample of AL07 follows the galactic field trend and is very different from the BS population found with *Gaia*. In total we identified 55 BS and five yellow straggler candidates.

Most of the BSs are within 0.5 mas yr^{-1} from the cluster mean, while only four candidates lie outside this region. The membership probabilities of the latter are 10%, 30%, 50%, and 70%. The remaining candidates have probabilities above 70%, so we decided to leave out all the stars with probability below 50% to define a bona fide, nonspurious BS population. The same criterion was applied to the yellow straggler candidates. From the five candidates, two stars lie outside the region mentioned above; they have membership probabilities of 30% and 40%, and were left out of our sample.

Summing up the results of this section, Collinder 261 has 53 BS and three YS candidates. These are listed in Table 3. When available, additional classification according to their binary nature, as reported in the astronomical database SIMBAD (Wenger et al. 2000), is also listed. The eclipsing, close binaries found among the

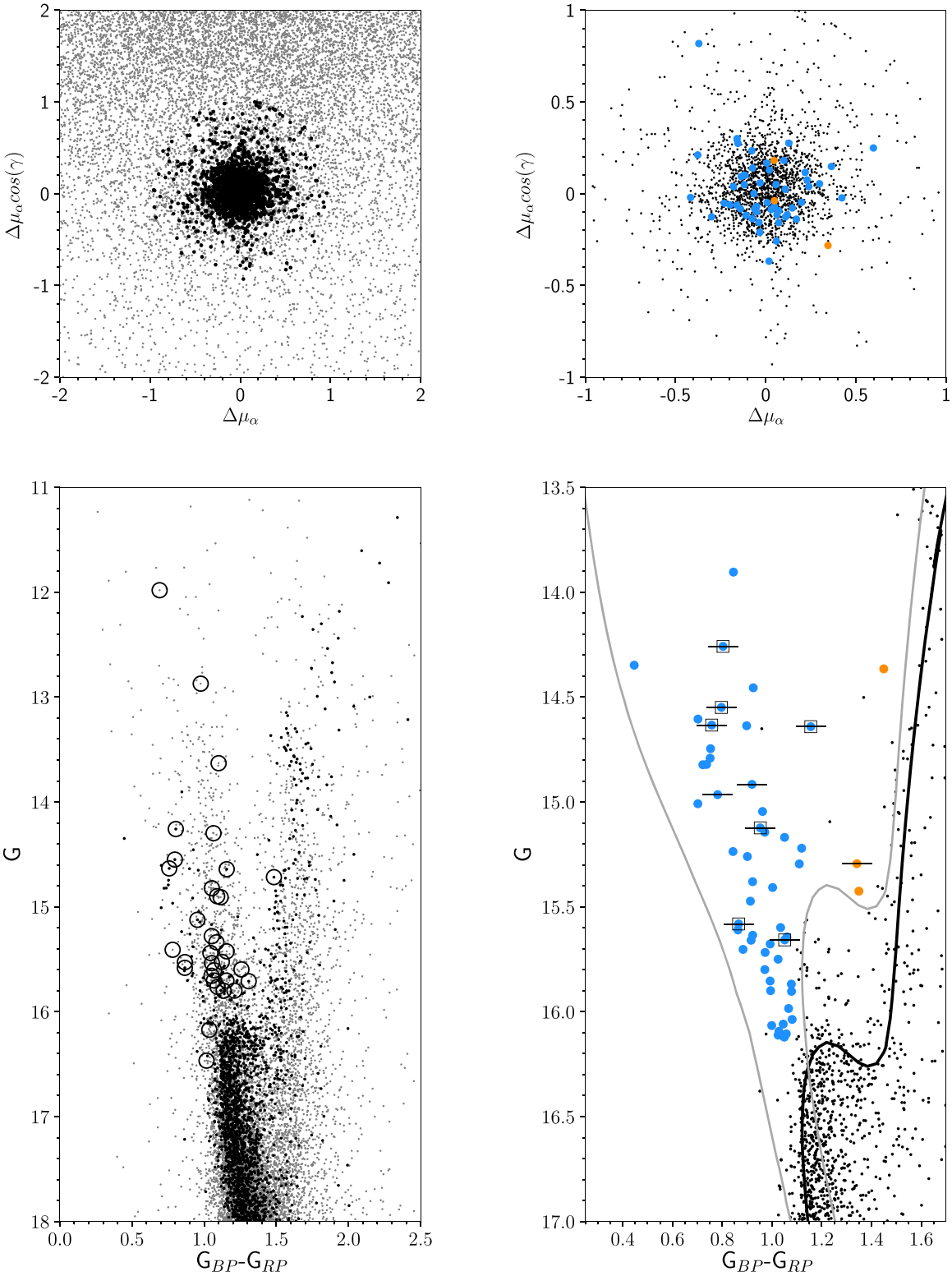

Figure 1. Upper panels: proper motions plane of Collinder 261. In the left panel, gray dots represent all the sources listed by *Gaia* DR2 within 15′ around the cluster center. Black filled circles are cluster members selected by Cantat-Gaudin et al. (2018). In the right panel, we display a zoom-in of the center of the plane; here, Collinder 261 members are the same as in the plot of the left, filled blue circles are BS candidates, and filled orange circles are yellow straggler candidates. Bottom panels: CMDs of Collinder 261. In the left panel, open black circles are BS candidates from Ahumada & Lapasset (2007). The right panel displays a zoom-in into the region of BSs; an isochrone from Bressan et al. (2012), shifted to the adopted cluster age and metallicity, is shown in black solid line. The ZAMS and the binary sequence are plotted as a gray solid line. Black squares are BSs already identified by Ahumada & Lapasset (2007). Stars with spectroscopic data are crossed with a horizontal line.

BSs of Collinder 261 are of the following types: β Lyrae, Algol, and W Ursae Majoris (W UMa). Binaries classified as β Lyrae are semidetached systems, i.e., one of the components of the pair is filling its critical Roche lobe, the stars are close enough that they are gravitationally distorted, and the periods are usually longer than 1 day. Algol variables are also semidetached binaries, whose

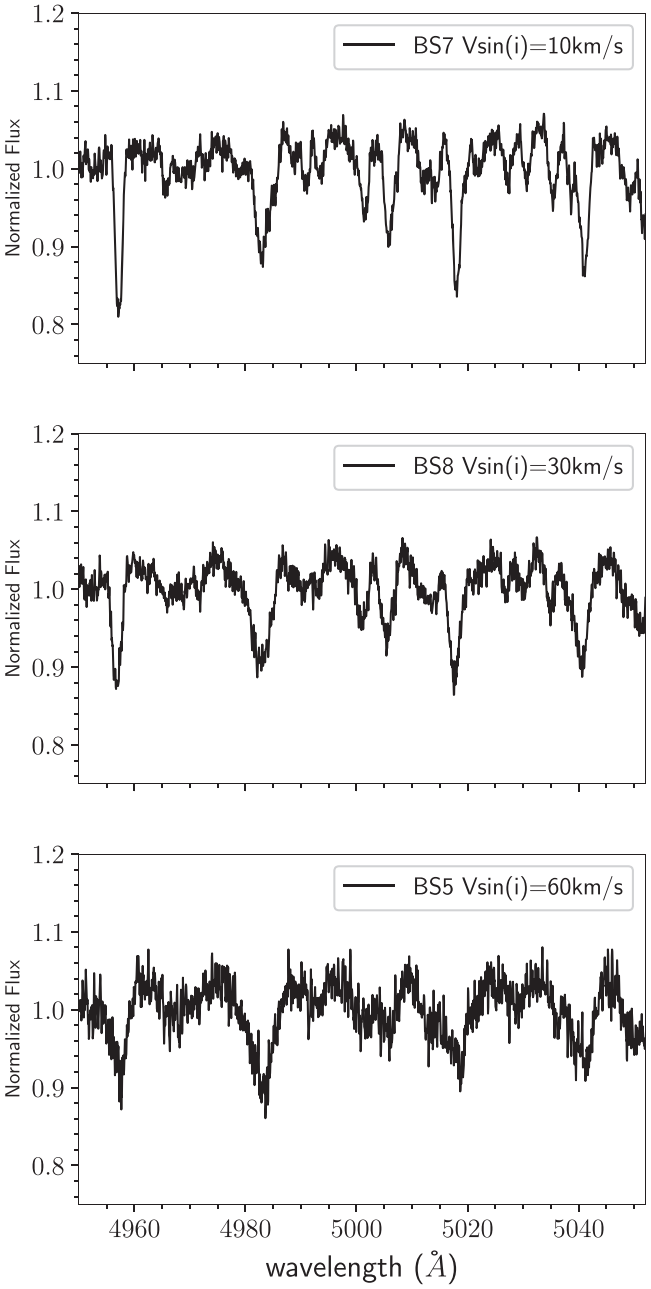

Figure 2. Examples of observed spectra for three BSs with different rotational velocities, labeled on each panel, in the wavelength range between 4950 and 5050 Å.

components have spherical or slightly ellipsoidal shapes. These stars have an extremely wide range of observed periods, from 0.2 to over 10,000 days. In the W UMa-type stars the components are in contact or almost in contact, and share a common envelope of material; the orbital period can be of just a few hours.

4. Spectroscopic Analysis

This is the first high-resolution spectroscopic analysis of the BS population in Collinder 261. Unfortunately, not all of the candidates were observed with FLAMES since, when we were allocated the observational time, we used the BS list of AL07 to select the targets, a list very different from that found in this work using *Gaia*. The spectroscopic analysis was carried out on

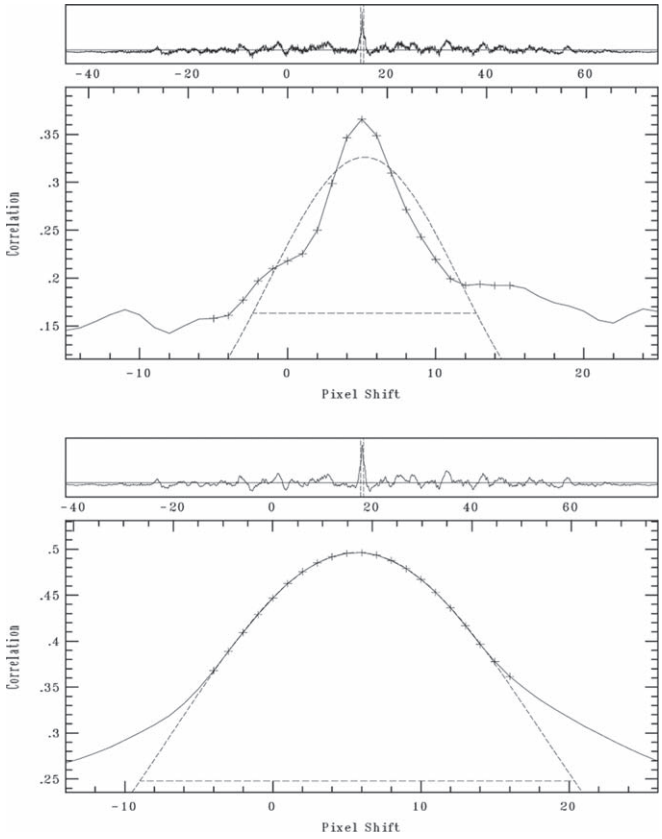

Figure 3. Cross-correlation peaks for star BS3, derived by the IRAF routine `fxcor`. The top panel shows one of the computed synthetic templates ($v\sin(i)$ equal to 10 km s^{-1}) cross-correlated with the spectrum of the star. Since the template is inadequate due to the low value of the rotational velocity, the cross-correlation curve is noisy. The bottom panel shows the same stellar spectrum cross-correlated with the correct template (with a rotational velocity of 30 km s^{-1}); in this case, the curve is smooth.

nine out of the 53 BSs in our list, and on one of the three YS candidates identified.

4.1. Radial Velocities

For each spectrum, radial velocities were determined with the IRAF `fxcor` cross-correlation task (Tonry & Davis 1979). Stellar spectra were cross-correlated with synthetic templates obtained with the SPECTRUM code[12] (Gray & Corbally 1994). Each synthetic spectrum was computed adopting the atomic and molecular data file `stdatom.dat`, which includes solar atomic abundances from Grevesse & Sauval (1998) and the line list `luke.lst`, suitable for mid-B- to K-type stars. Model atmospheres were calculated with the code ATLAS9 (Castelli & Kurucz 2003).

In Figure 2 we plotted, as an example, the spectra of three of our targets. The selection of a proper template for each star was mandatory because the targets have different rotational velocities (see Mucciarelli et al. 2014 for more information). We computed a set of templates with different rotational velocities $v\sin(i)$ ranging from 10 to 100 km s^{-1}, adopting the values: for the effective temperature, $T_{\rm eff} = 6000$ K, for the surface gravity, $\log g = 4.5$ cm s^{-2}, and for the microturbulence, $\xi = 0.0$ km s^{-1}. We carefully compared the spectrum of each star with the

[12] http://www.appstate.edu/~grayro/spectrum/spectrum.html

Table 3
Blue and Yellow Straggler Candidates from *Gaia* DR2 Data

Gaia DR2 Source Id.	G (mag)	G_{BP} (mag)	G_{RP} (mag)	$\mu_\alpha \cos(\delta)$ (mas yr^{-1})	μ_α (mas yr^{-1})	Parallax $\bar{\omega}$ (mas)	P_{Memb} (%)	Class[a]
5856432828647768960	15.00	15.28	14.57	−6.485 ± 0.038	−2.636 ± 0.043	0.304 ± 0.024	100	BS
5856437089255328384	15.23	15.57	14.73	−6.302 ± 0.050	−2.800 ± 0.044	0.372 ± 0.029	100	BS
5856511271928032256	14.74	15.03	14.28	−6.399 ± 0.037	−2.799 ± 0.041	0.318 ± 0.028	100	BS
5856530272864404224	15.40	15.80	14.80	−6.291 ± 0.052	−2.988 ± 0.052	0.306 ± 0.036	100	BS
5856527455365735680	15.26	15.61	14.71	−6.278 ± 0.053	−2.821 ± 0.056	0.290 ± 0.037	100	BS
5856516597687652352	15.89	16.31	15.31	−6.424 ± 0.057	−2.865 ± 0.068	0.295 ± 0.042	90	BS
5856527455365740032	15.16	15.59	14.54	−6.464 ± 0.042	−2.630 ± 0.042	0.337 ± 0.028	90	BS
5856527386646253312	14.54	14.85	14.05	−6.383 ± 0.034	−2.940 ± 0.036	0.297 ± 0.024	90	BS
5856527386646253440	15.12	15.45	14.50	−6.423 ± 0.043	−2.589 ± 0.055	0.333 ± 0.032	100	BS
5856527524085206656	13.90	14.24	13.39	−6.319 ± 0.030	−2.815 ± 0.030	0.297 ± 0.020	100	BS
5856517010004497792	15.65	16.03	15.11	−6.649 ± 0.053	−2.855 ± 0.060	0.340 ± 0.036	90	BS, EB β Lyrae
5856528348719355648	14.63	14.92	14.16	−6.388 ± 0.038	−2.886 ± 0.039	0.351 ± 0.026	100	BS
5856528623597294720	14.82	15.08	14.34	−6.766 ± 0.044	−2.751 ± 0.043	0.334 ± 0.032	70	BS
5856517078723954944	15.29	15.68	14.57	−6.489 ± 0.046	−2.813 ± 0.049	0.322 ± 0.032	100	BS
5856527558444960128	14.60	14.86	14.16	−6.110 ± 0.037	−2.691 ± 0.041	0.377 ± 0.026	100	BS
5856527455365743488	14.82	15.09	14.37	−6.427 ± 0.044	−2.495 ± 0.050	0.277 ± 0.033	100	BS
5856527661524172800	14.91	15.28	14.36	−6.343 ± 0.041	−2.564 ± 0.045	0.283 ± 0.028	100	BS, EB β Lyrae
5856527730243676800	15.60	15.94	15.07	−6.330 ± 0.055	−2.601 ± 0.051	0.331 ± 0.036	100	BS
5856528383078700288	15.71	16.11	15.14	−6.381 ± 0.059	−2.671 ± 0.063	0.281 ± 0.039	100	BS, EB Algol
5856528726676132096	15.85	16.23	15.24	−6.242 ± 0.060	−2.705 ± 0.063	0.345 ± 0.042	100	BS
5856528520517692032	15.64	16.06	15.00	−6.548 ± 0.059	−2.790 ± 0.053	0.320 ± 0.037	100	BS
5856528589237173120	15.22	15.65	14.53	−6.222 ± 0.046	−2.455 ± 0.047	0.374 ± 0.032	100	BS
5856529242072194816	15.65	16.09	15.04	−6.402 ± 0.063	−2.829 ± 0.060	0.310 ± 0.041	100	BS
5856517284882496128	14.63	15.00	14.10	−6.411 ± 0.037	−2.811 ± 0.038	0.268 ± 0.025	100	BS
5856528348719366528	15.47	15.83	14.91	−5.985 ± 0.052	−2.582 ± 0.054	0.344 ± 0.034	90	BS
5856515601255190272	14.25	14.57	13.76	−6.293 ± 0.031	−2.679 ± 0.033	0.313 ± 0.023	100	BS, EB Algol
5856514879700797696	14.34	14.49	14.05	−6.415 ± 0.032	−2.729 ± 0.035	0.322 ± 0.021	100	BS
5856528550550957184	14.96	15.25	14.47	−6.278 ± 0.043	−2.888 ± 0.042	0.281 ± 0.030	90	BS, EB Algol
5856529379511194240	14.79	15.07	14.32	−6.120 ± 0.038	−2.655 ± 0.039	0.297 ± 0.026	100	BS
5856527524085202048	15.58	15.90	15.04	−6.579 ± 0.051	−2.782 ± 0.051	0.307 ± 0.034	100	BS
5856432656849042688	16.03	16.50	15.41	−6.529 ± 0.068	−2.692 ± 0.060	0.290 ± 0.037	100	BS
5856420729693697408	16.12	16.57	15.52	−6.473 ± 0.064	−2.631 ± 0.064	0.334 ± 0.040	100	BS
5856419531427900672	15.90	16.36	15.28	−6.469 ± 0.059	−2.681 ± 0.059	0.304 ± 0.040	80	BS
5856437742090215680	15.79	16.20	15.22	−6.727 ± 0.069	−2.519 ± 0.055	0.245 ± 0.038	80	BS
5856436298981175168	16.09	16.52	15.49	−6.504 ± 0.064	−2.456 ± 0.057	0.343 ± 0.037	100	BS
5856436367700747392	15.98	16.43	15.37	−6.249 ± 0.073	−2.549 ± 0.066	0.436 ± 0.039	80	BS
5856483303104274560	15.12	15.54	14.57	−5.753 ± 0.047	−2.481 ± 0.040	0.403 ± 0.026	50	BS
5856512680677308160	16.10	16.55	15.49	−6.342 ± 0.065	−2.779 ± 0.270	0.270 ± 0.050	100	BS
5856528962867671936	16.06	16.46	15.46	−6.509 ± 0.075	−2.793 ± 0.069	0.204 ± 0.047	100	BS
5856528486157936384	16.05	16.47	15.42	−6.131 ± 0.071	−2.614 ± 0.064	0.412 ± 0.045	100	BS
5856528486157941376	16.11	16.52	15.50	−6.240 ± 0.074	−2.866 ± 0.066	0.320 ± 0.044	100	BS
5856527764603421184	15.86	16.31	15.23	−6.152 ± 0.073	−2.777 ± 0.062	0.278 ± 0.041	100	BS
5856529001554008064	14.64	15.12	13.97	−6.288 ± 0.037	−2.845 ± 0.040	0.306 ± 0.026	100	BS
5856528761035882496	15.38	15.74	14.82	−6.203 ± 0.053	−2.808 ± 0.053	0.226 ± 0.035	100	BS, EB W UMa
5856529276431965696	16.37	16.76	15.81	−6.194 ± 0.077	−2.974 ± 0.077	0.304 ± 0.053	100	BS
5856517211839051392	15.59	16.00	14.96	−6.721 ± 0.063	−1.912 ± 0.066	0.488 ± 0.043	70	BS
5856527558444963200	15.67	16.06	15.07	−6.231 ± 0.057	−2.845 ± 0.069	0.236 ± 0.038	100	BS
5856529276431950080	15.04	15.43	14.47	−6.460 ± 0.046	−2.848 ± 0.047	0.259 ± 0.031	100	BS
5856527558444950656	15.74	16.10	15.08	−6.052 ± 0.093	−2.676 ± 0.093	0.178 ± 0.062	100	BS
5856533326555127168	16.11	16.52	15.48	−6.332 ± 0.070	−3.098 ± 0.068	0.254 ± 0.047	100	BS
5856515665648722688	15.63	15.99	15.07	−6.180 ± 0.056	−2.869 ± 0.054	0.216 ± 0.038	100	BS, EB Algol
5856515669974676480	15.70	16.01	15.13	−5.928 ± 0.081	−2.753 ± 0.074	0.440 ± 0.056	90	BS
5856519037229366144	14.45	14.83	13.90	−5.575 ± 0.030	−2.430 ± 0.031	0.530 ± 0.021	80	BS
5856435130750056576	14.36	15.02	13.57	−6.005 ± 0.03	−3.012 ± 0.029	0.145 ± 0.018	60	YS
5856527622837778176	15.29	15.89	14.55	−6.302 ± 0.05	−2.768 ± 0.049	0.304 ± 0.033	100	YS
5856515601255187712	15.42	16.02	14.67	−6.304 ± 0.04	−2.549 ± 0.048	0.278 ± 0.033	100	YS

Note.
[a] Classification of the stars according to their binary nature, as reported in the astronomical database SIMBAD (Wenger et al. 2000).

templates, and we visually estimated the rotation rate from the profiles of the spectral lines. However, if the template had too low a rotational velocity, the shape turned out to be very noisy because the profiles of the lines and the spectrum noise were mapped together. In these cases, we had to increase the rotational velocity of the template for the cross-correlation procedure. The derived

Table 4
Individual Radial Velocity Measurements for the Blue and Yellow Stragglers in Our Sample

ID[a]	*Gaia* DR2 Source Id.	RV_1 (km s^{-1})	RV_2 (km s^{-1})	RV_3 (km s^{-1})	RV_4 (km s^{-1})	Classification[a]	$<v \sin(i)$ (km s^{-1})
BS1	5856527386646253312	−29.61 ± 3.69	−17.00 ± 3.39	+01.56 ± 2.61	−20.62 ± 4.61	M, CB	30
BS2	5856528348719355648	−26.09 ± 1.55	−26.21 ± 2.59	−24.39 ± 1.37	−25.46 ± 1.41	M	10
BS3	5856527524085202048	−24.23 ± 5.45	−17.25 ± 7.11	−00.02 ± 3.22	−02.55 ± 5.79	M, CB	30
BS4	5856528550550957184	−35.30 ± 8.45	−24.03 ± 11.07	−1.80 ± 6.59	−15.37 ± 6.72	M, CB	40
BS5	5856527661524172800	+12.44 ± 14.02	−05.36 ± 8.46	−38.77 ± 19.04	+19.70 ± 11.51	M, CB	60
BS6	5856527386646253440	−27.45 ± 5.14	−29.75 ± 3.30	−16.24 ± 3.31	−12.90 ± 3.35	M, LP	30
BS7	5856529242072194816	−24.08 ± 0.40	−24.30 ± 0.40	−24.02 ± 0.57	−23.91 ± 0.43	M	10
BS8	5856515601255190272	−35.96 ± 4.60	+10.20 ± 3.97	−63.48 ± 5.40	−66.91 ± 4.47	M, CB	30
BS9	5856529001554008064	−24.14 ± 0.76	−25.11 ± 0.86	−23.84 ± 1.11	−22.82 ± 0.74	M	10
YS1	5856527622837778176	−24.51 ± 0.34	−24.65 ± 0.34	−24.56 ± 0.30	−24.03 ± 0.45	M	10

Notes. Binary classification according with their radial velocity variability is reported in the last column.
[a] This work.

rates are considered as upper limits. An example of this procedure is illustrated in Figure 3.

The radial velocities measurements for the blue and yellow stragglers are reported in Table 4.

4.2. Errors

We consider the errors returned by `fxcor` as conservative estimates of the true uncertainties of the radial velocity. For each star we have four radial velocity measurements and `fxcor` error estimations. We computed the `fxcor` error for each star, and for each pair of measurements we calculated the radial velocity difference divided by the root square of 2. We then built the distribution histogram and fitted a Gaussian. We take the standard dispersion σ of the Gaussian as the true radial velocity error. We plotted the histograms together with the Gaussian fit and the true error in the upper panel of Figure 4. Additionally, we calculated the mean `fxcor` error for each rotational rate (estimated as we described above in Section 4.1). Our results are plotted in the bottom panel of Figure 4. The typical uncertainties for the slow rotators stars ($v \sin(i) = 10\,\mathrm{km\,s^{-1}}$) is about 1 $\mathrm{km\,s^{-1}}$. Stars rotating with velocities ranging approximately between 30 and 60 $\mathrm{km\,s^{-1}}$ have errors from 4 to 14 $\mathrm{km\,s^{-1}}$. Similar uncertainties values were found by Mucciarelli et al. (2014) on their BS sample. Therefore, we decided to adopt the `fxcor` error as a conservative estimation for the radial velocity uncertainty.

4.3. Membership and Evolutionary Status

Comparing our radial velocities with the mean value derived by Mishenina et al. (2015) for the clump stars, we can now try to determine the membership status of the objects in our sample. In what follows we will assume that BSs are the result of collisions, or that they are binary systems, with either relatively short periods (a few days or less) or rather long ones (about 1000 days). Tree epochs of observation are separated by a few days (∼6), and the fourth epoch is about 6 yr later. To assess membership, the radial velocities of the stars can be compared to the mean radial velocity of the cluster, taking into account the error bars—as derived in Section 4.1—and the possibility of binarity.

The TO mass of Collinder 261 is about 1.1 $M_\odot$ (Bragaglia & Tosi 2006); if the companions are MS stars, they have to be less massive since, by definition, they are the secondary components. If the systems are post-mass-transfer ones containing a white dwarf (e.g., Gosnell et al. 2014), then the mass of the companions are more likely peaked around 0.6 $M_\odot$, as found in NGC 188 (Geller & Mathieu 2011). We can thus

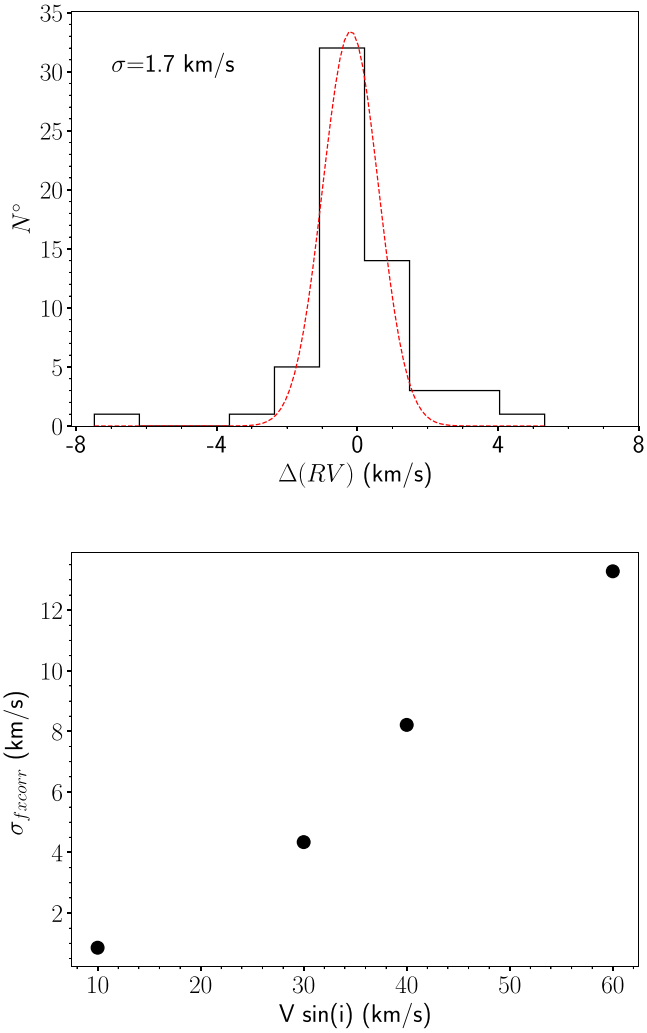

Figure 4. Upper panel: histogram of the differences—divided by the root square of 2—between pairs of radial velocities measurements for the same star. The best-fitting Gaussian to the distribution is plotted, and its standard deviation σ is indicated. Bottom panel: `fxcor` mean errors as a function of the upper rotational rates estimated in this work. See the text for details.

assume, for illustration purposes, that the binary would have a mass ratio of ∼0.5. For the system not to fill its Roche lobe—as this would imply a mass transferring system showing signs of accretion, which are not seen—the separation between the two stars should be larger than ∼3.5 $R_{\odot}$, with a minimal orbital period of the order of 0.5 days. In that case, the maximum orbital period would be 100 km s^{-1}. Thus, a star whose radial velocity differs from that of the cluster by up to 100 km s^{-1} could still be a member, if it were a close binary; in this case, however, we would expect that its radial velocity would change between two epochs. If we now consider the typical, post-mass-transfer, long-period binaries, with periods around 1000 days like those found to constitute the bulk of the BSs in NGC 188, we would expect a maximum radial velocity of 10–13 km s^{-1}. In this case, the difference in velocities between two epochs should be very small, i.e., below 1 km s^{-1}. Of course, it is possible to have a binary system in between these two cases. These considerations led us to define the following, rather conservative approach to confirm the membership of BS stars in Collinder 261.

1. If the individual radial velocities are, given their error bars, compatible with the cluster mean V_R, and do not change significantly over the four epochs, it is considered a possible single-star member, the outcome of a collision or a merger. It could of course also be a binary with a long period—greater than ∼1000 days. These stars are classified as "M."
2. On the other hand, if the individual radial velocities are, given their error bars, within 100 km s^{-1} with respect the cluster mean V_R, then the following occurs.
   (a) If the velocities differ more than 20 km s^{-1} from V_R and change significantly between two epochs, we can consider the star as a candidate for being a close-binary member of the cluster, "M, CB."
   (b) If the velocities are within 20 km s^{-1} from V_R and do not change by more than a few km s^{-1} between epochs (depending on the possible period, which is constrained by the difference with V_R), we possibly have a long-period member (period above 100 days): "M, LP."
3. The membership status of the binaries (CB and LP) can only be secured once we have determined the full orbital solution, and thus derived the systemic velocity. If none of the above apply, we consider the star to be a nonmember, "NM."

5. Results

5.1. Photometric Detections

We identified 53 possible BSs. Only six of them are similar to the BS population listed by AL07 for Collinder 261. Seven of our stars have already been noted as BSs and binaries in previous studies (Mazur et al. 1995; Vats & van den Berg 2017), see Table 3.

5.1.1. Radial Distribution

The BS radial distribution has been found to be a powerful tool to estimate the dynamical age of stellar systems (F12; Beccari et al. 2013). In fact, due to their masses—significantly larger than the average—and their relatively high luminosities, BSs are the ideal objects to measure the effect of dynamical processes, like dynamical friction and mass segregation (Mapelli et al. 2006). In order to investigate the cluster dynamical state, we studied the BS radial distribution and compared it to those of red giant branch (RGB), red clump (RC), and MS stars, taken as representatives of the normal cluster population, and that therefore are expected to follow the cluster distribution.

MS stars were selected from a region free of binary contamination. We considered as MS stars all those in the range of $17 < G < 18$. For RGB stars, we selected stars lying in the region $G_{\rm TO} < G < G_{\rm TO} - 2.5$, with $G_{\rm TO} \sim 16$ (see Figure 1). This allowed us to obtain a populous sample of reference stars in the same range of G magnitude of BSs, i.e., in the same degree of completeness. RC stars were selected from the region between $G_{\rm TO} - 2.5 < G < 13$. As we already mentioned, the accurate astrometric solutions of *Gaia* let us identify the stellar population of Collinder 261 in a very reliable way. We identified 53 BS, 79 RGB, 37 RC, and 833 MS stars.

The cumulative spatial distribution of the samples are shown in Figure 5, where the different panels show the normalized cumulative distribution of the BS candidates (black solid line), compared to those of MS stars (green dashed line), RGB stars (red dashed line), and RC stars (magenta dashed line). The BSs appear more centrally concentrated than the MS and RGB stars. The higher concentration of BSs that we find in the cluster internal region relative to the evolved stars has already been observed in other open clusters (Geller et al. 2008; Bhattacharya et al. 2019). The BS population in Collinder 261 is centrally concentrated, within about 5′ with respect to MS and RGB stars. In the right panel of Figure 5, clump stars and BSs have approximately the same distribution. In terms of mass segregation, BSs should be more centrally concentrated, given their combined masses—higher than that of TO stars, than RC stars—slightly less massive than TO stars. We suggest that the similarity of the radial profiles of BSs and RC stars is possibly due to the small number statistics in our sample for both populations. It is worth mentioning that Carraro et al. (2014) found marginal evidence that the BSs of the old open cluster Melotte 66 are more concentrated than its clump stars, as in Collinder 261.

To quantify whether the radial distributions of BS, RGB, RC, and MS stars are extracted from the same parent distribution, thus indicating an absence of segregation, we used the k-sample Anderson–Darling test (Scholz & Stephens 1987; hereafter A-D test). The A-D test is similar to the more widespread Kolmogorov–Smirnov test, but has a greater sensitivity to the tails of the cumulative distribution. The A-D test indicates a difference of 99.9% between the distributions of BS and MS stars, and a difference of 86.9% between the distributions of BS and RGB stars, which therefore favor the existence of a real mass segregation in Collinder 261. On the contrary, we do not find the population of BS stars to be centrally concentrated with respect to RC stars, as the A-D test gives a probability of 16.0% that both populations do not originate from the same distribution. The same observation was found by Carraro et al. (2014) in Melotte 66. Mazur et al. (1995) discovered 45 short-period eclipsing binaries in the Collinder 261 field, and estimated the frequency of the binary BSs among their sample within 6′ from the cluster center. They found a frequency of between 11% and 28%, supporting the

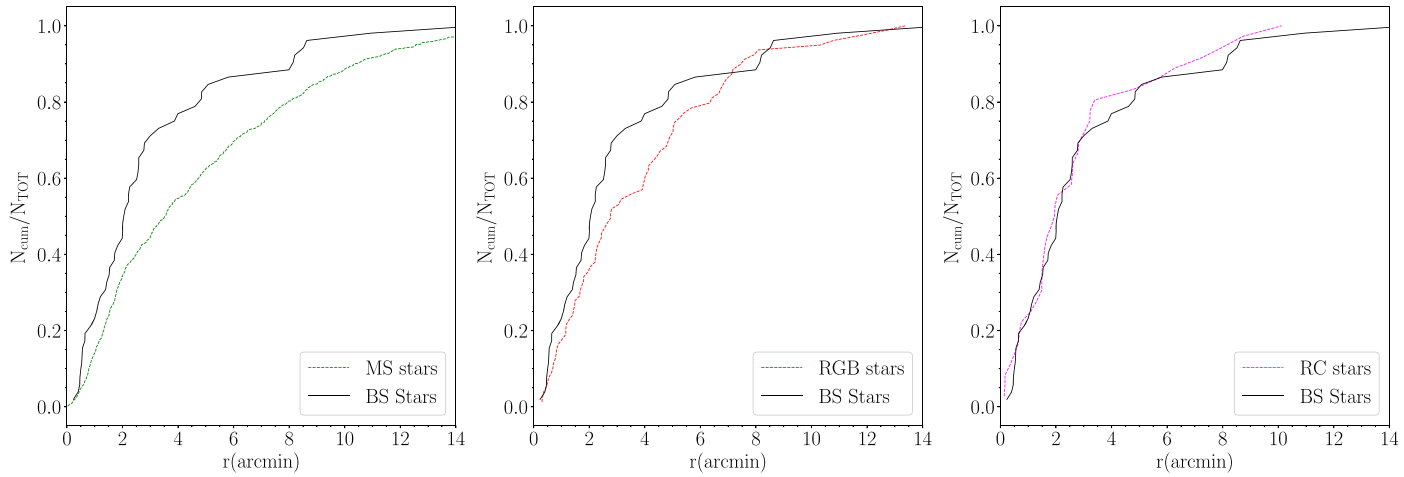

Figure 5. Cumulative spatial distribution of BSs (black solid lined), MS stars (green dashed lined), red giant stars (red dashed line), and clump stars (magenta dashed line) in Collinder 261.

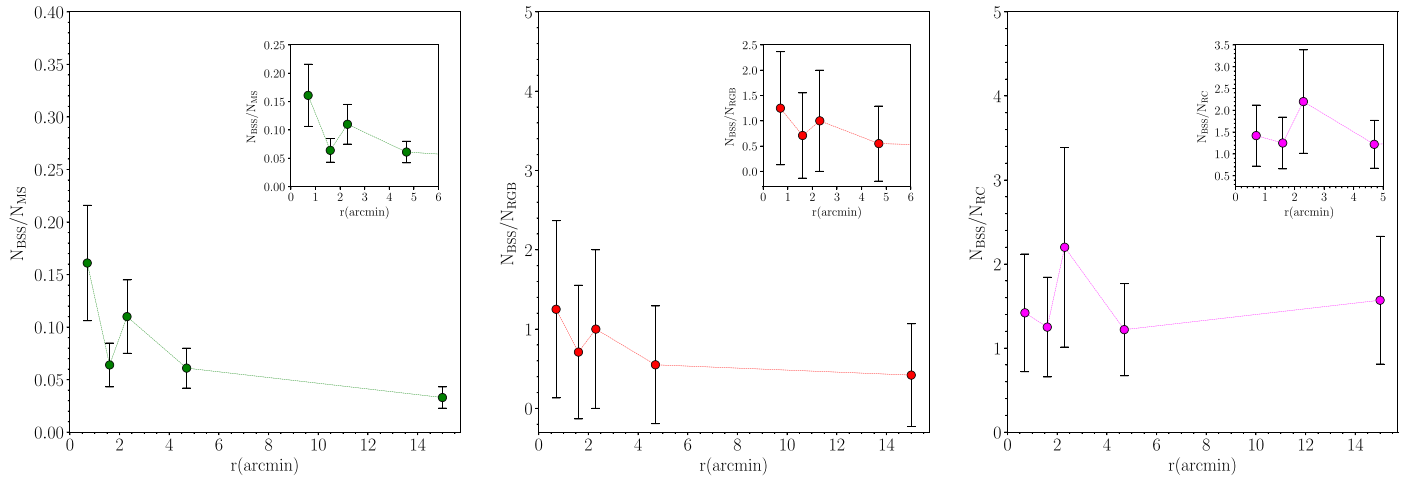

Figure 6. Number of BSs with respect to that of the reference stars: green for MS stars, red for red giant stars, and magenta for clump stars, plotted as a function of the distance from the cluster center expressed in arcmin. Errors are Poisson.

Table 5
Subpopulation Star Counts

Range (″)	N_{BS}	N_{MS}	N_{RC}	N_{RGB}	N_{BS}/N_{MS}	N_{BS}/N_{RC}	N_{BS}/N_{RGB}
0–42	10	62	7	8	0.161	1.42	1.25
42–96	10	156	8	14	0.064	1.25	0.71
96–138	11	100	5	11	0.110	2.20	1.00
138–282	11	179	9	20	0.061	1.22	0.55
282–900	11	326	7	26	0.033	1.57	0.42

hypothesis that a significant fraction of BSs formed as a result of mass transfer in close-binary systems. Our analysis also supports this scenario, in which BS stars in Collinder 261 are primordial binaries sinking toward the cluster center due to their combined mass, much larger than that of normal cluster stars.

A further indicator of segregation is the number of BSs normalized to the number of a reference population. We divided the field of view in five concentric annuli, each one containing approximately the same number of BSs (∼11). Star counts are in Table 5. Figure 6 plots the number of BS candidates with respect to that of reference stars in each annulus, as a function of the radial distance in arcmin, and the colors are the same as described above. When we compare the RC population and BS stars, we note a maximum at $r \sim 3'$ (see the right panel of Figure 6); however, when we consider the errors (Poisson errors) this peak disappears and the distribution becomes flat. The same behavior was observed when comparing BS with MS and RGB populations. Both ratios show a maximum value in the annuli closer to the center, followed by a minimum. The ratios within 6′ display two minima at $r \sim 2'$ and $r \sim 5'$, and two maximum peaks at $r \sim 1'$ and $r \sim 3'$. As in the previous case, these distributions

become flat considering the errors. A statistical test needs to be performed in the future, to evaluate the degree of BSs segregation with respect to the reference populations.

A cluster made up of stars of the same mass is dynamically relaxed on a timescale of $t_{\rm relax} \sim t_{\rm cross}\, N/6\log(N)$, where $t_{\rm cross} \sim D/\sigma_v$ is the crossing time, N is the total number of stars, and σ_v is the velocity dispersion (Binney & Tremaine 2008). The time $t_{\rm relax}$ is the characteristic scale in which the cluster reaches some level of kinetic energy equipartition with massive stars sinking to the core, and low-mass stars being transferred to the halo, so mass segregation in a star cluster scales with the relaxation time. Using the standard deviations of the projected proper motions ($\sigma_{\mu_\alpha} = 0.13$ mas yr^{-1} and $\sigma_{\mu_\alpha \cos(\delta)} \simeq 0.14$ mas yr^{-1}), and the sizes of the cluster core and half-mass–radius reported in Table 1, we obtain, for the cluster core, $t_{\rm relax,c} \sim 100$ Myr, and for the half-mass–radius $t_{\rm relax,h} \sim 250$ Myr. These values are significantly smaller than the estimated age of Collinder 261 (∼6–7 Gyr). Consequently, this could explain the presence of mass segregation in this cluster, particularly in the core.

We made and attempt to link our findings for Collinder 261 with those of F12 for GCs. We could not classify this cluster into any of the three families defined by F12 (Section 1), given the small number of BSs we have. Ferraro et al. (2012) discovered a tight anticorrelation between the core relaxation time and the shape of the radial distribution. Clusters with a flat distribution—i.e., that show no signs of segregation of its BSs—should have a relaxation time of the order of the age of the universe. Our findings do not match with their results, given that the small relaxation time we derive for the core of Collinder 261 is not compatible with a flat distribution.

5.2. Spectroscopic Detections

There are 10 stars in common between those observed with FLAMES and those in our proper motion and parallax selection. Out of our 53 BS candidates, only nine were observed with FLAMES. One yellow straggler candidate was also observed, and we decided to study its variability as well. Based on their radial velocity variations, we attempted to roughly assess their binary nature, namely, to decide if they may be close- or long-period binaries. Our results are plotted in Figure 7. All the probable binaries would need additional spectroscopic follow-up to be properly characterized, given the small number of observations. In total we found one long-period system, five close-binary systems, and three BS and one yellow straggler candidates without variations in their radial velocity measurements.

5.2.1. Long-period Binaries

Previous studies have revealed that the BS population in open clusters mostly contains long-period binaries (Geller et al. 2009). This kind of stars have periods ranging from a few days to decades, or even centuries, and it is very difficult to detect them spectroscopically and photometrically.

Star BS6 (%100) is a member according to our astrometric criteria and, according with Figure 7, is a possible long-period binary stars (M, LP) and is the only M, LP we found among our sample. This star is at 2′.55 from the cluster center.

5.2.2. Close Binaries

Stars BS1, BS3, BS4, BS5, and BS8 are cluster members and are also classified as possible close-binary systems (M, CB). The presence of these stars within the BS populations is quite unknown; according to previous studies performed in open clusters (OCs), they are less numerous than long-period binaries (e.g., NGC 188, Mathieu & Geller 2015; M67, Latham 2007), and their evolutionary histories involve dynamical encounters. According to Mazur et al. (1995), Collinder 261 is the star cluster that possesses the richest and most diversified population of short-period binaries found so far.

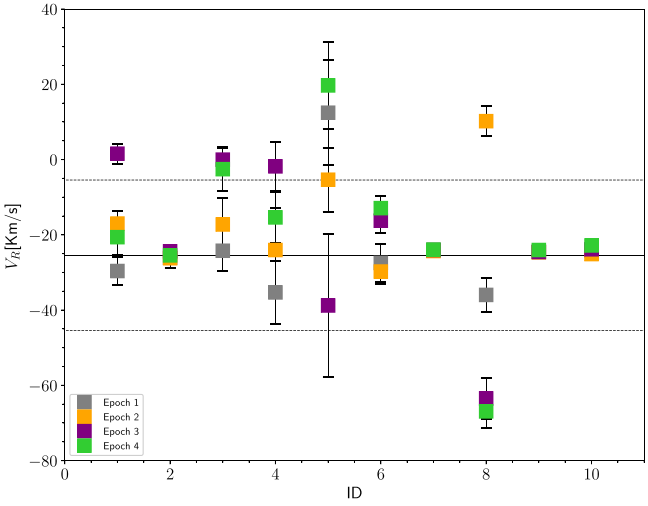

Figure 7. Radial velocity distribution of BS candidates in Collinder 261. Different colors indicate different epochs. The solid line represents the cluster mean radial velocity, while the two dashed lines indicate the ±20 km s^{-1} band we discuss in the text. Errors plotted are the values given by `fxcor`.

Stars BS1 (90%) and BS3 (%100) are at 2′.50 and 2′.58, respectively, from the cluster center.

Star BS4 (90%) has already been classified as an eclipsing binary of Algol type (i.e., detached; see Table 3). The All-Sky Automated Survey for Supernovae (ASAS-SN) Variable Stars Database[13] (Jayasinghe et al. 2019) gives an amplitude value of 1.87 mag. Mazur et al. (1995) give a period value of $P \sim 0.49135$ days. This star is at 0′.53 from the cluster center.

Star BS5 (100%) is a very well-studied member of Collinder 261. It has already been classified as a semidetached, eclipsing binary of β Lyrae type (Avvakumova et al. 2013). According to Samus et al. (2017) and Jayasinghe et al. (2019), this binary has a period P of ∼0.8040604 days and an amplitude of 0.44 mag. This star lies at 1′.70 from the cluster center and, according to its upper limit of $v \sin(i)$, it is a fast rotator (see Table 4).

Star BS8 (100%) is a completely different case. In the literature it has been cataloged as a detached, eclipsing binary of Algol type (Mazur et al. 1995; Avvakumova et al. 2013; Samus' et al. 2017), and also as a genuine BS according to AL07. Most Algol variables are quite close binaries, and therefore their periods are short, of typically a few days. Is also very well known that these stars are among the most active and X-ray luminous. Vats & van den Berg (2017) give an X-ray luminosity of $L_{X,u} \sim 8.05$ (unidades), and Mazur et al. (1995) a preliminary value of the period of $P \sim 2.11$ days. This star lies at 3′.29 from the cluster center.

5.2.3. Nonradial Velocity Variable BSs

There are three BSs in Collinder 261 that do not show significant radial-velocity variability: BS2 (100%), BS7 (100%),

[13] https://asas-sn.osu.edu/variables

and BS9 (100%). They lie at 1.′43, 0.′49, and 0.′46, respectively, from the cluster center. The upper limit we obtained for their rotational velocities are reported in Table 4. It is possible that these nonvelocity variable BSs are indeed long-period binaries, perhaps outside of our detection limit. Star BS2 is the bluest BS in our sample and BS7 is the reddest.

5.2.4. Yellow Straggler

Star YS1 (100%) is considered to be a yellow straggler according to its position in the CMD, and because it lies beyond the red limit ($G_{BP} - G_{RP}$) $\sim$ 1.2 for the BSs and red giants (see Section 3.1). This star is located at 1.′67 from the center.

5.3. Mass Estimations

We performed a mass estimation for BS4, BS5, and BS8. These stars are identified in the literature as eclipsing binaries, and are briefly described in Section 3.1. To fit the orbits we used the radial velocities we obtained in Section 4.1 and the periods reported in the literature (Section 5.2.2). For BS5 we divided the period by 2 (i.e., $P \sim 0.402$ days). For all stars we assumed that they are members, and that the mean velocity of the cluster is the systemic velocity γ of the binary.

To obtain the mass of the secondary (M_2) stars, we first estimated the masses of the primaries (M_1) from the CMD. The masses we finally derived for BS4 are $M_1 \sim 1.5\,M_\odot$ and $M_2 = 0.118 \pm 0.005\,M_\odot$, for BS5 are $M_1 \sim 1.51\,M_\odot$ and $M_2 = 0.21 \pm 0.01\ M_\odot$, and for BS8 are $M_1 \sim 1.51\ M_\odot$ and $M_2 = 0.42 \pm 0.02\,M_\odot$. Figure 8 shows the radial velocity curve for each star.

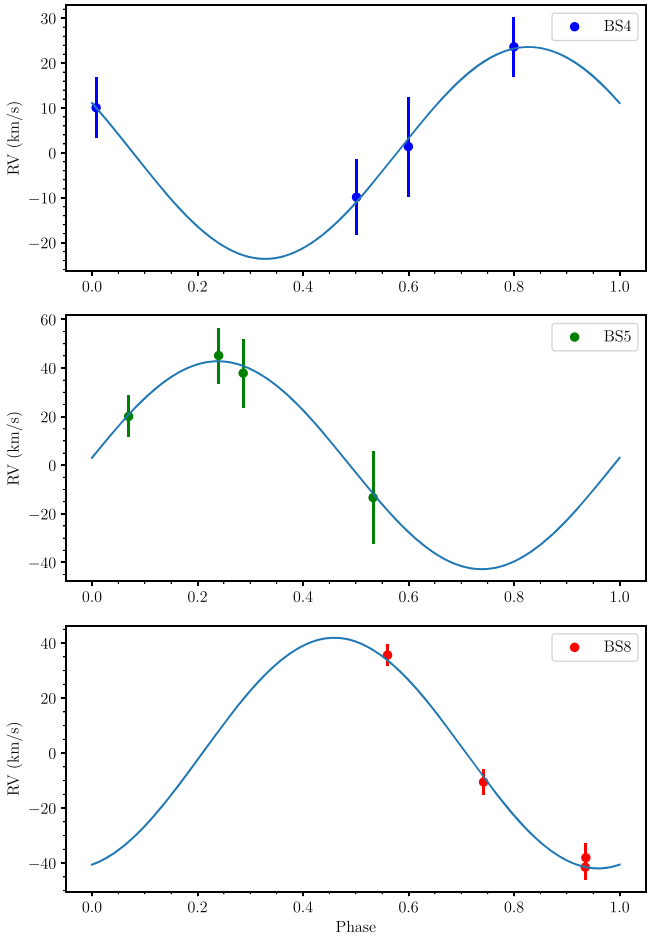

Figure 8. Radial velocity curves of BS4, BS5, and BS8.

6. Summary and Conclusions

With the accurate data available from the *Gaia* DR2 we have studied the BS population of the old open cluster Collinder 261. We found 53 BSs and three yellow stragglers among the cluster members. Using RC stars we calculated the mean proper motions and parallax values, and obtained $\mu_\alpha \cos\delta = -6.35 \pm 0.13$ mas yr^{-1}, $\mu_\alpha = -2.73 \pm 0.14$ mas yr^{-1}, and $\varpi = 0.321 \pm 0.019$ mas, in agreement with the literature. Our results are shown in Figure 1 and Table 3.

Following Bhattacharya et al. (2019), we used our candidates as test particles to probe the dynamical state of Collinder 261. In particular, we found that BSs are more centrally concentrated than RGB and MS stars (see Figure 5), and that they follow almost the same distribution than RC stars. To search for mass segregation, we normalized the BS population to several reference populations (RGB, MS, and RC stars; see Table 5); before each comparison, we performed an A-D test to check that the populations are not extracted from the same parent distribution, which should also indicate the presence of segregation. The test gives 99.9%, 86.9%, and 16.0% of MS, RGB, and, RC, respectively, that are not drawn from the same distribution than BSs. We found pronounced peaks and minima in the central regions of the cluster, similar to the ones found by Bhattacharya et al. (2019) in Berkeley 7. However, when taking into account the errors involved, these results were dismissed. We calculated the relaxation time of our cluster and found $t_{\mathrm{relax_c}} \sim 100$ Myr for the core, and $t_{\mathrm{relax_h}} \sim 250$ Myr for the half-light radius. Both values are quite small compared with the evolutionary age of our cluster (6–7 Gyr). Given these results, we were not able to place Collinder 261 in any of the families defined for GCs by Ferraro et al. (2012).

In the second part of the paper, we have presented the first high-resolution spectroscopic study of the BS population of Collinder 261, adopting membership criteria more solid than the simple photometric ones. So far, spectroscopic studies have been limited to a very small number of clusters. This is mostly because open clusters are believed to harbor many BS stars (Ahumada & Lapasset 2007), and therefore studying them in detail represents a huge observational challenge. The reason, however, for which they host so many BS stars, has not been fully deciphered yet. For this study we obtained four epochs of radial velocities; based on their variations, we separated these stars into candidate members, probable close binaries, and long-period binaries. All the probable binaries would need additional spectroscopic follow-up to be properly characterized, given the small number of epochs available. Unfortunately, the data that we have just presented cover only nine stars of the 53 possible BSs found in our analysis with *Gaia,* and one star of the three yellow straggler candidates we identified. This is so because we originally used the photometric-based list of Ahumada & Lapasset (2007) to select the objects to be observed with FLAMES, a list that differs significantly from that defined in this work.

Collinder 261 is a cluster of intermediate richness (see Figure 1). Our spectroscopic results are shown in Figure 7 and Table 4. Radial velocities for four epochs are available for 10 stars, among which we identified five as probable CB, and only

one as LP binaries. Four stars did not show radial velocity variations, among them one yellow straggler and three BSs. We performed an estimation of the masses of BS4, BS5, and BS8 from which we obtain $0.118 \pm 0.005\ M_{\odot}$, $0.21 \pm 0.01\ M_{\odot}$, and $M_2 = 0.42 \pm 0.02\ M_{\odot}$, respectively. We strongly suggest that at least one attempt to fit an orbit solution for the others BSs be made, since it will definitely help better understand the formation history and survival channels of BS stars.

We are grateful to the anonymous referee for the helpful comments which significantly helped improve the paper.

M.J.R. is supported by CONICY PFCHA through Programa de Becas de Doctorado en el extranjero- Becas Chile/2018-72190617.

S.V. gratefully acknowledges the support provide by Fondecyt reg. n. 1170518.

J.A. wishes to thank the ESO for stays in the Santiago Headquarters in 2010 January, 2011 November, and 2015 October, where part of this work was originally developed.

Software: IRAF, UPMASK (Krone-Martins & Moitinho 2014), Topcat, SPECTRUM (Gray & Corbally 1994), ATLAS9 (Castelli & Kurucz 2003).

ORCID iDs

M. J. Rain https://orcid.org/0000-0003-4009-8316
G. Carraro https://orcid.org/0000-0002-0155-9434
J. A. Ahumada https://orcid.org/0000-0002-7091-5025
S. Villanova https://orcid.org/0000-0001-6205-1493
H. Boffin https://orcid.org/0000-0002-9486-4840
L. Monaco https://orcid.org/0000-0002-3148-9836
G. Beccari https://orcid.org/0000-0002-3865-9906

References

Ahumada, J., & Lapasset, E. 1995, A&AS, 109, 375
Ahumada, J. A., & Lapasset, E. 2007, A&A, 463, 789
Aidelman, Y., Cidale, L. S., Zorec, J., & Panei, J. A. 2018, A&A, 610, A30
Arenou, F., Luri, X., Babusiaux, C., et al. 2018, A&A, 616, A17
Avvakumova, E. A., Malkov, O. Y., & Kniazev, A. Y. 2013, AN, 334, 860
Beccari, G., Dalessandro, E., Lanzoni, B., et al. 2013, ApJ, 776, 60
Bhattacharya, S., Vaidya, K., Chen, W. P., & Beccari, G. 2019, A&A, 624, A26
Binney, J., & Tremaine, S. 2008, Galactic Dynamics (2nd Ed.; Princeton, NJ: Princeton Univ. Press)
Bragaglia, A., & Tosi, M. 2006, AJ, 131, 1544
Bressan, A., Marigo, P., Girardi, L., et al. 2012, MNRAS, 427, 127
Boffin, H. M. J., Carraro, G., Beccari, G. et al. (ed.) 2015, in Ecology of Blue Straggler Stars: Astrophysics and Space Science Library, Vol. 413 (Springer: Berlin)
Brogaard, K., Christiansen, S. M., Grundahl, F., et al. 2018, MNRAS, 481, 5062
Cantat-Gaudin, T., Jordi, C., Vallenari, A., et al. 2018, A&A, 618, A93
Carraro, G., de Silva, G., Monaco, L., Milone, A. P., & Mateluna, R. 2014, A&A, 566, A39
Carraro, G., Vázquez, R. A., & Moitinho, A. 2008, A&A, 482, 777
Castelli, F., & Kurucz, R. L. 2003, in IAU Symp. 210, Modelling of Stellar Atmospheres, ed. N. Piskunov, W. W. Weiss, & D. F. Gray (Cambridge Univ. Press: Cambridge), A20
Dalessandro, E. 2014, in ASP Conf. Ser. 482, Tenth Pacific Rim Conference on Stellar Astrophysics, ed. H. W. Lee, Y. W. Kang, & K. C. Leung (San Francisco, CA: ASP), 257
de Marchi, F., de Angeli, F., Piotto, G., Carraro, G., & Davies, M. B. 2006, A&A, 459, 489
De Silva, G. M., Freeman, K. C., Asplund, M., et al. 2007, AJ, 133, 1161
Dias, W. S., Alessi, B. S., Moitinho, A., & Lepine, J. R. D. 2002, A&A, 389, 871
Evans, D. W., Riello, M., De Angeli, F., et al. 2018, A&A, 616, A4
Ferraro, F. R., Lanzoni, B., Dalessandro, E., et al. 2012, Natur, 492, 393
Gaia Collaboration, Brown, A. G. A., Vallenari, A., et al. 2018, A&A, 616, A1
Gaia Collaboration, Prusti, T., de Bruijne, J. H. J., et al. 2016, A&A, 595, A1
Gao, X.-h. 2018, PASP, 130, 124101
Geller, A. M., Hurley, J. R., & Mathieu, R. D. 2010, in IAU Symp. 266, Star Clusters: Basic Galactic Building Blocks throughout Time and Space, ed. R. de Grijs & J. R. D. Lepine (Cambridge: Cambridge Univ. Press), 258
Geller, A. M., Hurley, J. R., & Mathieu, R. D. 2013, AJ, 145, 8
Geller, A. M., & Mathieu, R. D. 2011, Natur, 478, 356
Geller, A. M., & Mathieu, R. D. 2012, AJ, 144, 54
Geller, A. M., Mathieu, R. D., Harris, H. C., & McClure, R. D. 2008, AJ, 135, 2264
Geller, A. M., Mathieu, R. D., Harris, H. C., & McClure, R. D. 2009, AJ, 137, 3743
Gosnell, N. M., Mathieu, R. D., Geller, A. M., et al. 2014, ApJL, 783, L8
Gosnell, N. M., Mathieu, R. D., Geller, A. M., et al. 2015, ApJ, 814, 163
Gozzoli, E., Tosi, M., Marconi, G., & Bragaglia, A. 1996, MNRAS, 283, 66
Gray, R. O., & Corbally, C. J. 1994, AJ, 107, 742
Grevesse, N., & Sauval, A. J. 1998, SSRv, 85, 161
Hills, J. G., & Day, C. A. 1976, ApJL, 17, L87
Hurley, J., & Tout, C. A. 1998, MNRAS, 300, 977
Jayasinghe, T., Stanek, K. Z., Kochanek, C. S., et al. 2019, MNRAS, 486, 1907
Jordi, C., Gebran, M., Carrasco, J. M., et al. 2010, A&A, 523, A48
Kaluzny, J. 1994, AcA, 44, 247
Katz, D., Sartoretti, P., Cropper, M., et al. 2019, A&A, 622, A205
Krone-Martins, A., & Moitinho, A. 2014, A&A, 561, A57
Latham, D. W. 2007, HiA, 14, 444
Latham, D. W., & Milone, A. A. E. 1996, in ASP Conf. Ser. 90, The Origins, Evolution, and Destinies of Binary Stars in Clusters, ed. E. F. Milone & J. C. Mermilliod (San Francisco, CA: ASP), 385
Leonard, P. J. T. 1996, ApJ, 470, 521
Lindegren, L., Hernández, J., Bombrun, A., et al. 2018, A&A, 616, A2
Luo, Y.-P. 2015, RAA, 15, 733
Mapelli, M., Sigurdsson, S., Ferraro, F. R., et al. 2006, MNRAS, 373, 361
Mathieu, R. D., & Geller, A. M. 2009, Natur, 462, 1032
Mathieu, R. D., & Geller, A. M. 2015, ASSL, 413, 29
Mazur, B., Krzeminski, W., & Kaluzny, J. 1995, MNRAS, 273, 59
McCrea, W. H. 1964, MNRAS, 128, 147
Mishenina, T., Gorbaneva, T., Pignatari, M., Thielemann, F.-K., & Korotin, S. A. 2015, MNRAS, 454, 1585
Mucciarelli, A., Lovisi, L., Ferraro, F. R., et al. 2014, ApJ, 797, 43
Pribulla, T., Rucinski, S., Matthews, J. M., et al. 2008, MNRAS, 391, 343
Samus', N. N., Kazarovets, E. V., Durlevich, O. V., Kireeva, N. N., & Pastukhova, E. N. 2017, ARep, 61, 80
Scholz, F. W., & Stephens, M. A. 1987, J. Am. Stat. Assoc., 82, 918
Tonry, J., & Davis, M. 1979, AJ, 84, 1511
Vats, S., & van den Berg, M. 2017, ApJ, 837, 130
Wenger, M., Ochsenbein, F., Egret, D., et al. 2000, A&AS, 143, 9